Analyst

PAPER

View Article Online
View Journal | View Issue

Cite this: *Analyst*, 2018, **143**, 3570

Thermosensitive molecularly imprinted core–shell CdTe quantum dots as a ratiometric fluorescence nanosensor for phycocyanin recognition and detection in seawater†

Jinhua Li,[a] Junqing Fu,[b] Qian Yang,[a] Liyan Wang,[a] Xiaoyan Wang[a,c] and Lingxin Chen *[a,d,e]

Received 1st May 2018,
Accepted 17th June 2018

DOI: 10.1039/c8an00811f

rsc.li/analyst

Versatile molecular imprinted fluorescence sensors have been prepared for various species, but the imprinting based fluorescence detection of target proteins upon different external stimulation is rarely reported. Herein, a novel phycocyanin-imprinted ratiometric fluorescence nanosensor was developed for the temperature regulated sensing and detection of a phycocyanin target based on fluorescence resonance energy transfer (FRET). The nanosensor was fabricated *via* simple facile copolymerization, with amino/carboxyl modified quantum dots (QDs) as a fluorescent support, *N*-isopropylacrylamide as a thermo-responsive functional monomer, *N*,*N*-methylenebisacrylamide as a cross-linker and phycocyanin as a template. Under temperature control at 20 °C and 45 °C, the fluorescence intensities of the QDs and phycocyanin were regularly decreased and enhanced, respectively, to a different extent as the concentration of phycocyanin increased, and thereby the ratio of the two fluorescence peak emission intensities of QDs and phycocyanin was used to determine the concentration of phycocyanin. Good linearity was obtained within the range of 0–1.8 μM (r = 0.9900) with a low detection limit of 3.2 nM, and excellent recognition selectivity towards the phycocyanin target was achieved over other proteins. Moreover, satisfactory recoveries of 92.0–106.8% were obtained in spiked seawater samples. This study provides a facile, fast and intelligent way to conduct identification analysis of trace proteins in complex water matrices, and can push forward protein imprinting and stimuli-responsive imprinting related research.

Introduction

Nowadays, cyanobacterial blooms pose a great threat to water bodies, aquatic animals and human health, due to their potential to induce water intake pollution, hypoxia, biodiversity reduction and toxic secondary-metabolite production.[1] Phycocyanin, an accessory cyanobacteria-specific pigment protein, often provides quantitative information relating to cyanobacterial bloom assessment, owing to its close relationship with cyanobacterial biomass.[2] So, phycocyanin in cyanobacteria can be used as an indicator for cyanobacteria, which is of great significance for marine environmental monitoring.[3] Moreover, phycocyanin can emit fluorescence with a high absorption coefficient over a wide spectral range, and it has high biological and biomedical value and is stable in water for a long time.[2,4] However, to the best of our knowledge, few measurement methods have been developed for phycocyanin determination, except for remote sensing methods,[1,5,6] and imprinting sensing methods.[4,7–9] Therefore, it is highly important to develop sensitive, selective, and rapid, as well as low-cost and environment-friendly, methods to identify and detect phycocyanin.

Molecular imprinting, used for preparing molecularly imprinted polymers (MIPs), is a promising approach for the realization of the selective detection of template analytes, especially trace analytes in complex matrices, owing to the MIP tailor-made binding sites, which are complementary to the template molecules in size, shape, and functional groups.[10] Recently, stimulus-responsive MIPs (SR-MIPs) have aroused increasing interest for their controllable molecular recognition

[a]*CAS Key Laboratory of Coastal Environmental Processes and Ecological Remediation, Yantai Institute of Coastal Zone Research, Chinese Academy of Sciences, Yantai 264003, China. E-mail: lxchen@yic.ac.cn; Tel: +86-535-2109130*
[b]*The Provincial Food and Drug Inspection Institute of Shandong, Jinan 250101, China*
[c]*School of Pharmacy, Binzhou Medical University, Yantai 264003, China*
[d]*College of Chemistry and Chemical Engineering, Yantai University, Yantai 264005, China*
[e]*College of Chemistry and Chemical Engineering, Qufu Normal University, Qufu 273165, China*

†Electronic supplementary information (ESI) available. See DOI: 10.1039/c8an00811f

upon specific external cue changes, such as temperature, pH, ionic strength, and so on.[10,11] Amongst SR-MIPs, temperature-/thermo-responsive MIPs (T-MIPs) can not only respond to external temperature changes, but they also have molecular recognition ability for template molecules, providing a promising strategy for ensuring the system can respond more rapidly to an external temperature change.[11] The template molecules can be more easily removed from or rebind to T-MIPs *via* appropriately regulating the environmental temperature, which will enhance mass transfer and rebinding percentages.[11] Moreover, the temperature regulation system is simple, convenient, cost-effective and environment-friendly.[12] Accordingly, T-MIPs are widely being researched.[10–13] For instance, Xiong *et al.*[12] proposed switchable zipper-like T-MIPs, using 2-acrylamide-2-methylpropanesulfonic acid (AMPS) as a thermoresponsive monomer for controlled adsorption with the release of estradiol (E2) in response to temperature change, with which higher adsorption capacity and stronger selectivity were obtained at 30 °C compared to at 20 °C and 40 °C. Besides AMPS, *N*-isopropylacrylamide (NIPAM) is more widely used as a thermo-responsive monomer in T-MIP preparation because of its lower critical solution temperature (LCST), between 25 °C and 32 °C, permitting applications at physiological temperatures, with a promising future.[14] At its LCST, NIPAM possesses soluble (hydrophilic)–insoluble (hydrophobic) transition properties, displaying a coil (soluble) state when the solution temperature is below the LCST, as well as a collapsed (insoluble) state above the LCST.[15] Pan *et al.*[16] reported a lysozyme-imprinted nanogel, using NIPAM as the major monomer for the specific recognition and controlled release of proteins. However, most of these reported T-MIPs rely on bound/free separation and subsequent chromatographic analysis, making the experimental procedure tedious and real-time monitoring unachievable. Hence, molecular imprinted sensing materials are preferred for instantaneous phycocyanin determination. For better transduction of binding events into measurement signals, an ideal alternative is to combine these with ultra-sensitive detection technology, *e.g.*, fluorometry.

The combination of fluorescence detection and MIPs for phycocyanin determination has been explored, depending on the red-emitting autofluorescence of phycocyanin.[4,17] However, separation between bound/free phycocyanin is still required in order to distinguish the fluorescence signals produced by the MIP-phycocyanin complex and free molecules in test solution. To eliminate the separation procedure, an alternative is to introduce proper fluorescence materials (not existing in test samples) during MIP preparation, to produce an optical signal upon phycocyanin recognition. For example, embedding quantum dots (QDs) into mesoporous structured MIPs and then interacting these with phycocyanin to cause QD fluorescence quenching is a good choice.[7] Besides, combining the luminescence of embedded fluorescence substances and the intrinsic luminescence of phycocyanin is a potential way to propose a ratiometric fluorescence sensor, which can exhibit two emission bands.[8] The ratio of the two fluorescence intensities, instead of the absolute intensity of one peak, can be utilized for the determination of phycocyanin. And therefore, owing to this self-referencing capability, compared with traditional fluorescence measurements with a sole responsive signal, ratiometric fluorescence sensors exceed in not being affected by interference from various experimental factors, such as the instrumental conditions, background interference and operational parameters, providing more precise measurements.[8,18–20] What's more, ratiometric fluorescence sensors tend to provide different colors upon target recognition at different concentrations, facilitating visual detection even without using any analytical instruments.[8,18–20]

So in the present work, we propose a novel thermosensitive molecular imprinting based ratiometric fluorescence nanosensor for phycocyanin detection *via* facile one-pot free radical polymerization. The nanosensor was produced *via* the copolymerization of the thermosensitive functional monomer NIPAM and the cross-linker *N*,*N*-methylenebisacrylamide (MBA) in the presence of phycocyanin on the surface of QDs. The wide excitation but sharp and symmetrical emission spectrum of QDs, differing from phycocyanin, has a part that overlaps with the absorption spectrum of phycocyanin, which enables fluorescence resonance energy transfer (FRET). Consequently, a phycocyanin-imprinted ratiometric fluorescence sensor was developed for the temperature regulated sensing detection of the phycocyanin target based on FRET; that is, the fluorescence intensities of QDs and phycocyanin themselves changed upon different degrees of phycocyanin rebinding, under the modulation of temperature. The constructed sensor was well validated and successfully applied to seawater samples.

Experimental

Reagents and materials

Glutathione (GSH), *N*-isopropylacrylamide (NIPAM), *N*,*N*-methylenebisacrylamide (MBA), and bovine serum albumin (BSA) were purchased from Sigma-Aldrich (Shanghai, China). Phycocyanin, phycoerythrin, and spirulina powder were kindly provided by Shandong Oriental Ocean Co. (Yantai, China). Tellurium powder, chloride cadmium ($CdCl_2$), sodium borohydride ($NaBH_4$), potassium peroxydisulfate ($K_2S_2O_8$), sodium hydroxide (NaOH), ammonia, hydrochloric acid (HCl), thioglycollic acid (TGA), and ethanol were supplied by Sinopharm Chemical Reagent Co. Ltd (Shanghai, China). All chemicals were of at least analytical grade and used as received without further purification, unless otherwise specified. All aqueous solutions throughout this work were prepared with ultrapure water (18.2 MΩ specific resistance), which was produced using a Pall Cascada laboratory water system (Millipore, Bedford, MA, USA).

Surface seawater samples from the Fisherman's Wharf of the Yellow Sea, located in the coastal zone area of Yantai City (Yantai, China), were gathered in a Teflon bottle and stored at 4 °C before use. The water samples were simply filtrated

through 0.45 μm PTFE syringe filters (Phenomenex, Los Angeles, CA, USA) to remove suspended particles before MIP treatment.

Synthesis and surface modification of CdTe QDs

Water-soluble TGA–GSH modified CdTe QDs were synthesized according to a reported method,[21] with some necessary modifications. Briefly, 68.4 mg of $CdCl_2 \cdot 2H_2O$, 25 μL of TGA, 0.11 g of GSH and 75 mL of ultrapure water were mixed to form the cadmium precursor. The mixture was adjusted to pH 9 with 1 M NaOH and stirred for 30 min under N_2 conditions. Then, 1 mL of freshly prepared NaHTe supernatant (prepared by the orderly adding of 1.5 mL of alcohol and 0.5 mL of water into a mixture of 38.3 mg of tellurium powder and 40 mg of $NaBH_4$, with fast sealing and heating at 40 °C for 4 h) was injected into the cadmium precursor solution, with N_2 deaerating for 20 min. The reaction solution was heated until boiling and refluxed for 2 h, and the resultant product was TGA–GSH modified CdTe QDs.

Preparation of the thermosensitive molecular imprinted sensor

Firstly, 6 mL (20 mg) of the above-obtained TGA–GSH modified CdTe QDs and 10 mL of phycocyanin (2 g L^{-1}) were dispersed into 14 mL of water under stirring for 2 h. Next, 6 mL of aqueous solution containing 100 mg of NIPAM and 80 mg of MBA was added into the above solution. After deaerated with N_2, polymerization was initiated by adding 4 mg of KPS and reacting for 4 h at 30 °C. The resultant products were centrifuged and washed to remove the templates using ethanol/NaOH (5 : 1, v/v), followed by ethanol and ultrapure water washing to neutrality for further use. Accordingly, a thermosensitive molecular imprinted sensor was attained, which was named MIP sensor for simplicity. For comparison, a non-imprinted polymer (NIP) sensor was also prepared as above without adding phycocyanin.

Characterization

Morphological evaluations were conducted using transmission electron microscopy (TEM, JEM-1230, operating at 100 kV). A Fourier transform infrared (FT-IR) spectrometer (Thermo Nicolet Corporation, USA) was employed to record the infrared spectra of samples, using a pressed KBr tablet method. UV-vis spectra were obtained using a Thermo Scientific NanoDrop 2000/2000C spectrophotometer (Thermo Fisher Scientific, Waltham, MA). All fluorescence measurements were obtained using a Fluoromax-4 spectrofluorometer (Horiba Scientific) under the same conditions: the excitation and emission slit widths were both 3 nm and the excitation wavelength was set to 468 nm for the QDs and 590 nm for phycocyanin, respectively.

Temperature control experiments

The temperature responsiveness evaluation of the MIP sensor was performed as follows. 0.8 mg of MIP was dispersed in 2 mL of phycocyanin solutions of different concentrations (0, 0.25, 0.50, 0.70, 0.90, 1.4, and 1.8 μM), and then these were immediately transferred into thermostat water baths adjusted to 20 °C and 45 °C, respectively, and incubated for 10 min. Subsequently, the solutions were immediately transferred into the fluorometer for fluorescence measurements. Each group of experiments was carried out five times in parallel.

Results and discussion

The construction and possible detection method of the thermosensitive imprinted ratiometric fluorescence sensor

Fig. 1 illustrates the construction process and possible detection method of the thermosensitive phycocyanin imprinted ratiometric fluorescence sensor. Firstly, the 555 nm emitting CdTe QDs were modified with GSH and TGA for surface passivation and the achievement of desirable amino and carboxyl

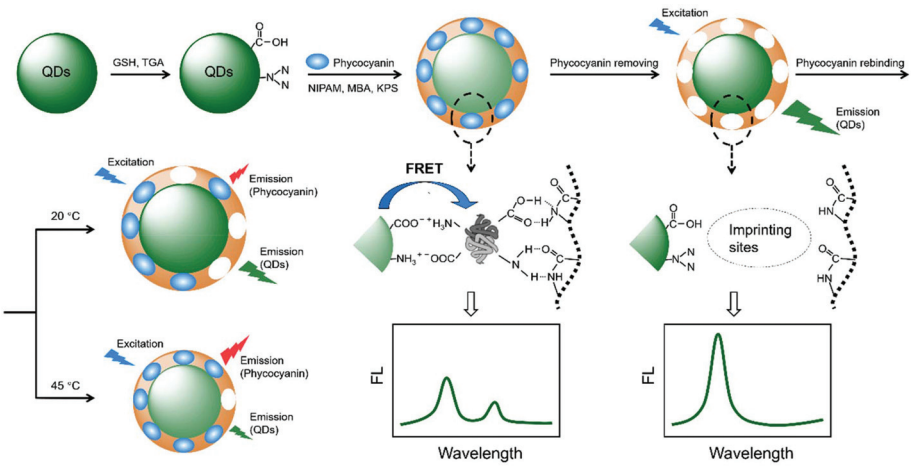

Fig. 1 A schematic illustration showing the construction and recognition process and possible detection method of the thermosensitive imprinted ratiometric fluorescence sensor (MIP sensor) for phycocyanin.

groups for MIP anchoring, where TGA and GSH are widely used modifiers/stabilizers because of the carboxyl, amino, and amide coordination groups, and the complexation reaction between the thiol group and Cd^{2+}.[22] Besides, modification with TGA and GSH can better coat QDs to reduce their toxicity. Then, the modified QDs were used as fluorescent supports, with NIPAM as a thermo-responsive functional monomer, MBA as a cross-linker and phycocyanin as a template; spontaneously copolymerization was initiated by KPS, leading to the formation of MIPs with the subsequent removal of the phycocyanin template. The MIP shell layer could not only protect the QD fluorescence and effectively decrease the QD toxicity but it could also facilitate high accessibility to binding sites and the rapid mass transfer of template molecules.[23] Upon light irradiation, only one QD fluorescence emission peak was observed at 561 nm, with a small red shift compared with the initial spectrum. However, after rebinding phycocyanin through hydrogen bonds, the QD fluorescence intensity was quenched and the intensity of phycocyanin was enhanced through FRET from the energy donor of the QDs to the acceptor of phycocyanin, realizing the ratiometric determination of phycocyanin. Moreover, the MIPs could achieve different sensing abilities with temperature changes owing to the transition property of NIPAM: the coil (soluble) state at low temperatures and the collapsed (insoluble) state at high temperatures correspond to opened and blocked channels, respectively, so the amount of phycocyanin getting to recognition sites was modulated.

FRET could reasonably explain the corresponding fluorescence quenching and enhancement in the QDs and phycocyanin, respectively. As seen in Fig. S1,† the emission spectrum of the QDs overlaps with the absorption spectrum of phycocyanin, meeting the prerequisite demands of FRET and allowing the QDs to act as an energy donor and phycocyanin to act as an acceptor.[24] When phycocyanin bound again into the imprinted sites, its spatially close interaction with the QDs conformed to the distance requirements between a donor and an acceptor (within 10 nm).[20,24,25] Hence, the fluorescence emission of the QDs could be strongly absorbed by the rebound phycocyanin, resulting in fluorescence quenching of the donor and enhancement of the acceptor. However, free phycocyanin in test solution, owing to the wider distance between and unsatisfactory orientation of the donor and acceptor dipoles, couldn't be excited through absorbing energy from the QDs or by excitation light at 468 nm, and further failed to emit fluorescence. So, only the rebound phycocyanin could be detected; that is, the constructed thermosensitive imprinted ratiometric fluorescence sensor could recognize and detect phycocyanin based on FRET.

The optimization of experimental conditions for MIP sensor construction

In order to attain the optimal construction conditions for the MIP sensor, the dosage of modified QDs, the binding of the thermosensitive monomer NIPAM and the type/amount of elution solvent were investigated, as below.

Binding experiments with 10 mg (3 mL), 15 mg (4.5 mL), 20 mg (6 mL) and 30 mg (9 mL) of QDs and 20 mg of phycocyanin (10 mL) were carried out. Using the same reagents and conditions, the results showed that a small amount of QDs not only exhibited low fluorescence intensity, but also made it difficult to form a shaped particle; excessive QDs did not increase the fluorescence intensity. Furthermore, fluorescence quenching experiments on the QDs were carried out using a fixed dosage of QDs (400 μg, 120 μL) and various amounts of phycocyanin (0, 100, 200, 300, 400 and 500 μg, *i.e.*, 0, 50, 100, 150, 200, and 250 μL). As seen in Fig. S2A,† the quenched amount of QDs increased with an increase in the amount of phycocyanin until they reached the same amounts (400 μg). Obviously, more phycocyanin, 500 μg, did not quench more QDs. So, combining the quenching results, and with the purpose of saving QDs, the same amounts of phycocyanin and QDs, 400 μg, were used to construct the expected MIP sensor. That is, 200 μL (2 g L^{-1}) of phycocyanin and 120 μL of QDs were selected for MIP sensor construction.

The appropriate amount of NIPAM was selected as 1.5 mg when the phycocyanin mass was fixed at 400 μg, as verified using the fluorescence spectra shown in Fig. S2B.† As seen, at a fixed phycocyanin concentration, the fluorescence intensity of phycocyanin gradually decreased as NIPAM increased (0, 0.5, 1.0, 1.5 and 2.0 mg), indicating that phycocyanin and NIPAM formed a stable host–guest interaction. However, when more than 1.5 mg of NIPAM was present, only a small intensity decrease was observed, suggesting that additional NIPAM did not contribute to the formation of a more stable complex. Given the fact that inadequate NIPAM couldn't provide enough sites to enhance the sensitivity, but that an excess of NIPAM would generate unspecific adsorption so that selectivity would be decreased, 2.0 mg of NIPAM was chosen in the present work.

Additionally, as listed in Table S1,† the eluting effects of several reported eluents were investigated. Compared with others, the eluent ethyl alcohol/NaOH (5 : 1, v/v) was preferred because it provided the obvious fluorescence peak of the MIPs after elution, with easy dispersion and centrifugation, as well as high MIP yield.

Characterization of the MIP sensor

The constructed MIP sensor was characterized *via* TEM, fluorescence spectra and FT-IR. As shown in Fig. 2, the average particle diameters of the CdTe QDs (Fig. 2A) and MIPs (Fig. 2B and inset) were about 5 nm and 30–40 nm, respectively. The obvious difference in size demonstrated the copolymerization of phycocyanin, NIPAM and MBA onto the surfaces of the QDs. The morphological imperfection of the spherical MIPs may be caused by the small particle size of the QDs, so most of the imprinted layers were wrapped on unevenly assembled QDs.[25–27] Despite this, the size of 30–40 nm still largely decreased mass transfer resistance and made imprinted sites more accessible, which played a beneficial role in the sensing and recognition of the imprinted materials.

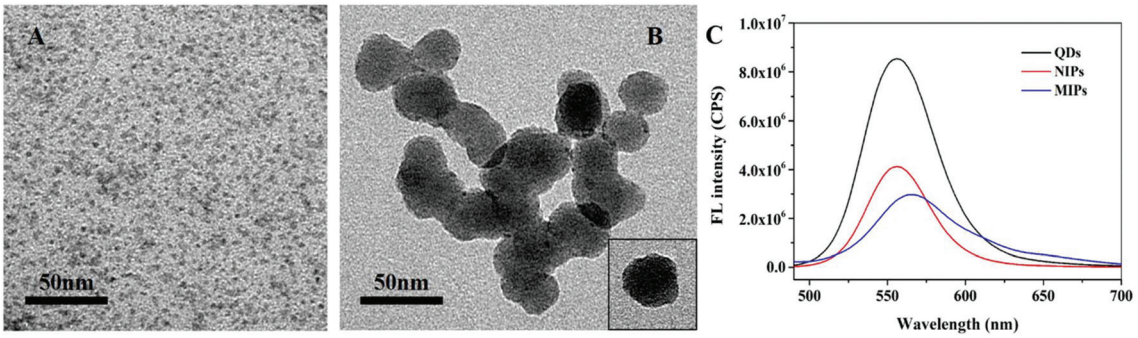

Fig. 2 TEM images of (A) CdTe QDs and (B and inset) MIPs, and (C) fluorescence spectra of the QDs, NIPs and MIPs (1.26 mg mL^{-1}) at 20 °C.

Additionally, fluorescence spectra of QDs, NIPs and MIPs at the same concentration were observed at room temperature, as shown in Fig. 2C. Obviously, the intensities of the MIPs and NIPs were weaker than that of the QDs, owing to the quenching effect of the polymer layers on the QDs, and the former had a distinct red shift of about 6 nm. The red shift could be attributed to the formation of a hybrid MIP structure, which could increase the effective size of the QDs and reduce the quantum size effect, leading to a red shift in the photoluminescence maximum. The lower fluorescence intensity of the MIPs than the NIPs, similar to that previously reported,[28–31] is very likely owing to the effect of residual template molecules in the MIPs, since the absolutely complete removal of template molecules is almost impossible.[10,28–31] On the other hand, the results also could indicate that the imprinting of phycocyanin has taken place successfully.

The differences in FT-IR spectra (Fig. 3) confirmed the characteristic functional group changes between the QDs and the MIPs before and after phycocyanin rebinding. As seen in Fig. 3, the characteristic peaks around 1643 cm^{-1} and 3432 cm^{-1} of the three samples were all strong, and could be ascribed to the bending vibration of N–H, which proved that amino groups were induced successfully. The ionic R-COO^- at 1396 cm^{-1} in the QDs was stronger than that in the MIPs and the MIPs rebinding to phycocyanin, possibly owing to the coverage of the imprinted layer. The characteristic absorption peaks at 1535 cm^{-1} and 1650 cm^{-1} could be assigned to amido bonds, and the peak intensities of MIPs rebinding to phycocyanin were stronger than those of MIPs, which demonstrated that phycocyanin was successfully rebound, because the protein contains abundant peptide bonds. Therefore, a phycocyanin imprinted sensor was obtained.

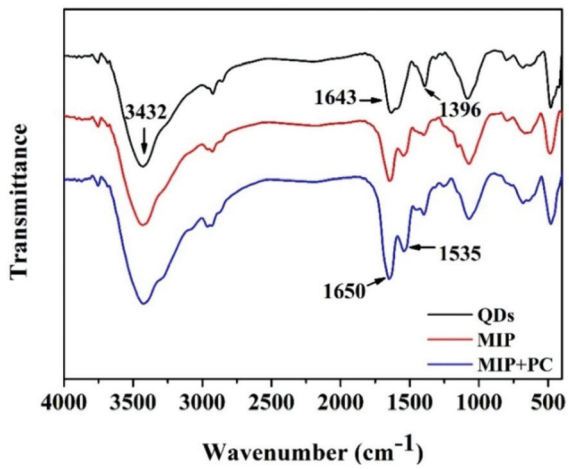

Fig. 3 FT-IR spectra of modified QDs, and MIPs before and after PC (phycocyanin) rebinding.

Intelligent response to different temperatures

As is well known, poly-NIPAM is able to change its structure and size upon changes in the environmental temperature:[13,32] it becomes soluble when the temperature is below its LCST because the intermolecular hydrogen bonds are dominant, while the relative equilibrium of hydrophilicity/hydrophobicity is lost when temperature is above its LCST.[33] Hence, the obtained MIPs were promising candidates to show this temperature sensitivity characteristic. As proof-of-concept, after adding phycocyanin, the fluorescence intensities of the thermo-responsive MIPs were measured under the same conditions, only with different temperatures of 20 °C and 45 °C, standing for low and high temperature, respectively. As seen in Fig. 4A, the interaction of the MIPs with phycocyanin showed a conspicuous temperature-dependent on–off fluorescence intensity, indicating that poly-NIPAM contracted at the high temperature of 45 °C, thereby blocking partial channels in the sensor; however, at the low-temperature of 20 °C the poly-NIPAM was relaxed and the channels opened, hence, imprinted sites were accessible to phycocyanin, leading to a fluorescence intensity change. Additionally, the fluorescence intensities of the MIPs after adding phycocyanin at low and high temperatures were recorded continuously for four cycles, as displayed in Fig. 4B. As seen, the fluorescence intensities recorded at both 20 °C and 45 °C showed no significant decrease after the four-cycle test, suggesting the temperature-dependent recognition ability of the thermo-responsive MIPs was quite stable and reliable.

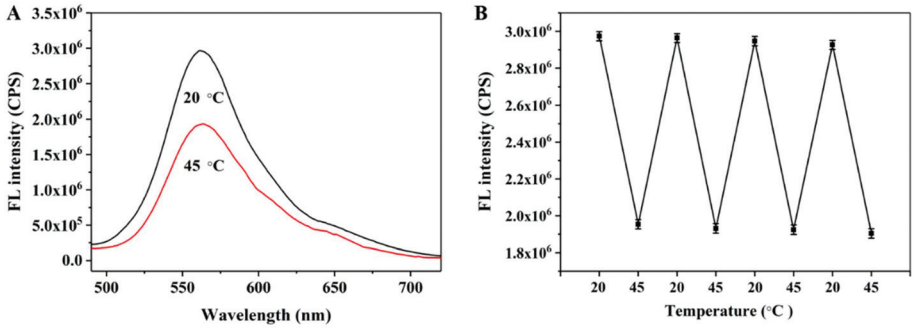

Fig. 4 (A) Fluorescence spectra of the MIP sensor at 20 °C and 45 °C, and (B) the recoverability of the fluorescence intensity of the MIP sensor between 20 °C and 45 °C, respectively, through four repeated examinations. The concentration of MIPs was 1.26 mg mL^{-1}.

The response time, sensitivity and selectivity of the MIP sensor

For excellent sensing performance, a quick response, high sensitivity and super selectivity are matters of necessity. The response time of the MIP sensor to phycocyanin was first investigated. As shown in Fig. 5A, after adding phycocyanin, the fluorescence intensity of the MIP sensor at 561 nm gradually decreased as the time increased and it then obtained a constant value within 10 min. That is, most of the imprinted cavities were situated at the surface or in the proximity of the surface, so this largely decreased mass transfer resistance and made imprinted sites accessible, and dynamic adsorption equilibrium with the free phycocyanin in the test solution could be reached within a short time. Hence, 10 min was chosen as the response time for further experiments.

For sensitivity evaluation, the fluorescence response was investigated based on the change in the fluorescence intensity ratio (I_{655}/I_{561}) upon adding different amounts of phycocyanin into the MIP dispersion solution at 20 °C or 45 °C. As displayed in Fig. 5B and C, in the absence of phycocyanin at 20 °C or 45 °C, only one fluorescence peak from the QDs was observed at 561 nm; as the phycocyanin concentration increased from 0 to 1.8 μM, the fluorescence intensity of the QDs was remarkably quenched along with the fluorescence

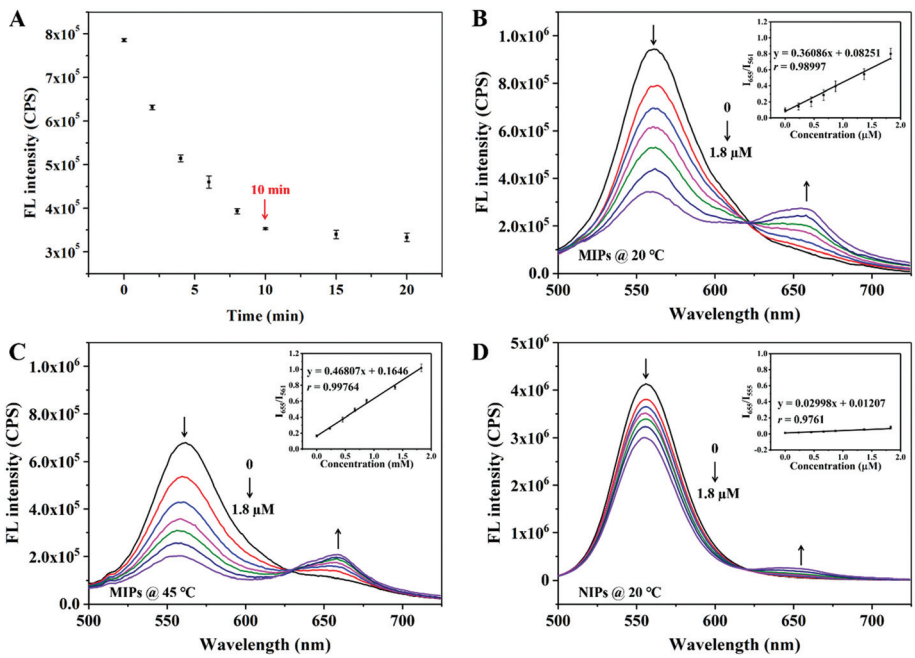

Fig. 5 (A) Fluorescence intensity changes upon increasing the response time of MIPs to phycocyanin, and fluorescence spectra (B–D) of the MIP sensor (B, C) upon the addition of the indicated concentrations of phycocyanin at temperatures of (B) 20 °C and (C) 45 °C, respectively, and of the NIP sensor (D) upon the addition of the indicated concentrations of phycocyanin at a temperature of 20 °C. The inset plots (B–D) shows the linear relation between I_{655}/I_{561} (B, C) or I_{655}/I_{555} (D) and the concentration of phycocyanin, from 0 to 1.8 μM. The concentration of MIPs or NIPs was 0.40 mg mL^{-1}.

intensity of phycocyanin at 655 nm being enhanced. This indicated that FRET occurred and the emission energy of the QDs was absorbed by phycocyanin. For more directly observing the fluorescence response upon the addition of phycocyanin, a calibration curve was established through plotting the intensity ratio *versus* the phycocyanin concentration (insets of Fig. 5B and C). As seen, I_{655}/I_{561} increased regularly as the phycocyanin concentration increased and, at both 20 °C and 45 °C, excellent linearity was attained ranging from 0 to 1.8 μM. The limit of detection (LOD), defined as $3\sigma/s$, where σ is the standard deviation of the blank signal and s represents the slope of the calibration curve, was calculated to be 3.2 nM. In particular, the trend of the ratio increasing at 45 °C (0.46807) was larger than at 20 °C (0.36086), indicating that the thermosensitive functional monomer NIPAM changed its properties and resultantly changed the sensing performance of the MIPs.

Besides, the sensing performance of the NIPs towards phycocyanin was also investigated. As shown in Fig. 5D and its inset, the change in I_{655}/I_{555} was largely smaller than it was for the MIPs, *i.e.*, the sensitivity of the NIPs to phycocyanin was less positive. We define the imprinting factor as the ratio of the slopes of the two calibration curves of the MIPs and NIPs, and hence, high imprinting factors of 12.1 and 15.6 could be obtained at 20 °C and 45 °C, respectively. We could reasonably conclude that the obvious gap in sensitivity was caused by the matching degree between phycocyanin and the recognition sites of the MIPs or NIPs. Abundant phycocyanin-complementary recognition sites were located on the nanosized MIPs and it was easy for the MIPs to capture phycocyanin and change their fluorescence characteristics; however, no recognition sites existed in the NIPs and only non-specific binding caused a slight variation in the fluorescence intensity.

Furthermore, the selectivity of the sensor towards phycocyanin was investigated using phycoerythrin, spirulina powder and BSA as control proteins. The concentration of these four proteins was set to 1.368 μM and the ratios of the fluorescence intensities ($I_{655}/I_{561\ \text{or}\ 555}$) of the MIPs and NIPs before and after the proteins were added were recorded. As shown in Fig. 6, for the MIP sensor, the change in the ratio upon phycocyanin rebinding was considerably larger than that caused by the other three proteins. Due to the fact that phycoerythrin has a similar spatial structure to phycocyanin, and both exist in the spirulina power, phycoerythrin and spirulina powder also changed the fluorescence intensity ratio, obviously to a larger extent than BPA, which possesses a completely different shape and molecular weight to phycocyanin. We ascribed this result to the shape, size and functional group memory of the imprinted cavities with regards to phycocyanin, rather than towards the other proteins.[34] Additionally, no obvious changes in the fluorescence intensity ratios were found after the addition of these four proteins to the NIPs. To sum up, the results implied the high selectivity of the MIPs towards phycocyanin.

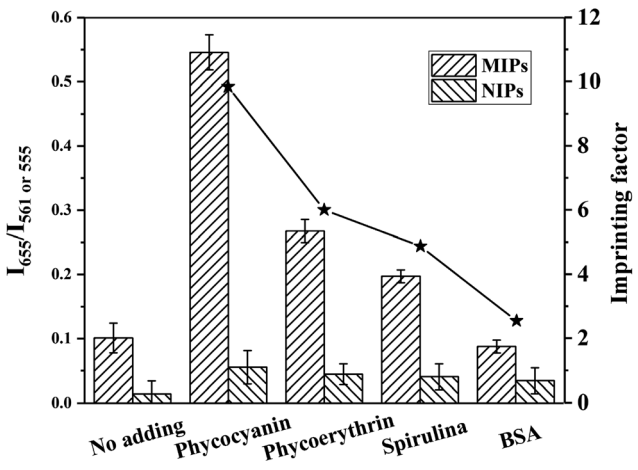

Fig. 6 The selectivity of the MIPs and NIPs for phycocyanin over other analogues, including phycoerythrin, spirulina and BSA at a concentration of 1.368 μM at 20 °C.

Sensor stability and practical applications

To assess the fluorescence stability of the MIP sensor, the fluorescence intensity at the maximum emission peak was measured repeatedly every 10 min. As exhibited in Fig. S3,† the fluorescence of the MIP sensor was quite stable within 60 min, indicating that the MIPs were uniformly dispersed in solution without obvious settlement and agglomeration. What's more, with storage in a refrigerator at 4 °C without exposure to light, the modified QDs could be kept for at least 6 months, and the fluorescence intensity of the MIP sensor could be maintained within 90% in an initial one month, proving good physical stability and chemical inertness owing to the highly cross-linked polymeric features. Hence, the imprinted sensor had good stability and could be used as an excellent sensor for protein detection.

To demonstrate its practical application, the MIP sensor was further employed for the determination of phycocyanin in real seawater samples spiked with different concentrations of phycocyanin (0.25, 0.50, 0.75 and 1.00 μM). Each concentration was analyzed using five replicates, and the averages were presented with relative standard deviation (RSD) values. As listed in Table S2,† satisfactory recoveries were obtained in the range of 92.0–106.8%, with RSDs of 2.9–5.5%, indicating that the obtained MIP sensor was practically applicable for the accurate determination of trace phycocyanin in complicated seawater samples.

Conclusions

In summary, stimulus-responsive materials, molecular imprinting techniques and ratiometric fluorescence detection were smartly integrated to construct a novel thermosensitive imprinted ratiometric fluorescence nanosensor *via* a facile method for the temperature-regulated sensing recognition and detection of phycocyanin, based on FRET. The sensor demonstrated an excellent temperature response, high sensitivity and

selectivity, good stability and reliability, and great application potentials. The simple, rapid, reliable, time-saving and cost-effective strategy could offer an excellent fluorescence analysis platform for phycocyanin monitoring, and an alternative approach for the construction of FRET-based detection systems. Furthermore, the development of such types of MIP based sensors with temperature-modulated functionality can provide convenient and environmentally friendly ways to conduct contaminant analysis and environmental monitoring, and satisfy green sustainable development goals.

Conflicts of interest

There are no conflicts to declare.

Acknowledgements

This work was supported by the National Natural Science Foundation of China (21477160, 41776110), the Natural Science Foundation of Shandong Province of China (ZR2016BL25, ZR2016DB07), the National Defence Science and Technology Innovation Project of the Chinese Academy of Sciences (CXJJ-16M254), and the Department of Science and Technology of Shandong Province of China (GG201709290055).

Notes and references

1 B. Q. Qin, W. Li, G. W. Zhu, Y. L. Zhang, T. F. Wu and G. Gao, Cyanobacterial bloom management through integrated monitoring and forecasting in large shallow eutrophic lake Taihu (China), *J. Hazard. Mater.*, 2015, **287**, 356–363.

2 L. Qi, C. Hu, H. Duan, J. Cannizzaro and R. Ma, A novel MERIS algorithm to derive cyanobacterial phycocyanin pigment concentrations in a eutrophic lake: theoretical basis and practical considerations, *Remote Sens. Environ.*, 2014, **154**, 298–317.

3 S. Nagaoka, K. Shimizu, H. Kaneko, F. Shibayama, K. Morikawa, Y. Kanamaru, A. Otsuka, T. Hirahashi and T. Kato, A novel protein C-phycocyanin plays a crucial role in the hypocholesterolemic action of spirulina platensis concentrate in rats, *J. Nutr.*, 2005, **135**, 2425–2430.

4 Z. Zhang, J. H. Li, J. Q. Fu and L. X. Chen, Fluorescent and magnetic dual-responsive coreshell imprinting microspheres strategy for recognition and detection of phycocyanin, *RSC Adv.*, 2014, **4**, 20677–20685.

5 K. S. Song, L. Li, Z. C. Li, L. Tedesco, B. Hall and K. Shi, Remote detection of cyanobacteria through phycocyanin for water supply source using three-band model, *Ecol. Inform.*, 2013, **15**, 22–33.

6 S. Mishra, D. R. Mishra, Z. Lee and C. S. Tucker, Quantifying cyanobacterial phycocyanin concentration in turbid productive waters: a quasi-analytical approach, *Remote Sens., Environ.*, 2013, **133**, 141–151.

7 Z. Zhang, J. H. Li, X. Y. Wang, D. Z. Shen and L. X. Chen, Quantum dots based mesoporous structured imprinting microspheres for the sensitive fluorescent detection of phycocyanin, *ACS Appl. Mater. Interfaces*, 2015, **7**, 9118–9127.

8 X. Y. Wang, J. L. Yu, Q. Kang, D. Z. Shen, J. H. Li and L. X. Chen, Molecular imprinting ratiometric fluorescence sensor for highly selective and sensitive detection of phycocyanin, *Biosens. Bioelectron.*, 2016, **77**, 624–630.

9 B. W. Li, Z. Zhang, J. Qi, N. Zhou, S. Qin, J. Choo and L. X. Chen, Quantum dot-based molecularly imprinted polymers on three-dimensional origami paper microfluidic chip for fluorescence detection of phycocyanin, *ACS Sens.*, 2017, **2**, 243–250.

10 L. X. Chen, X. Y. Wang, W. H. Lu, X. Q. Wu and J. H. Li, Molecular imprinting: perspectives and applications, *Chem. Soc. Rev.*, 2016, **45**, 2137–2211.

11 S. F. Xu, H. Z. Lu, X. W. Zheng and L. X. Chen, Stimuli-responsive molecularly imprinted polymers: versatile functional materials, *J. Mater. Chem. C*, 2013, **1**, 4406–4422.

12 H. H. Xiong, X. Q. Wu, W. H. Lu, J. Q. Fu, H. L. Peng, J. H. Li, X. Y. Wang, H. Xong and L. X. Chen, Switchable zipper-Like thermoresponsive molecularly imprinted polymers for selective recognition and extraction of estradiol, *Talanta*, 2018, **176**, 187–194.

13 W. Zhang, W. Liu, P. Li, H. B. Xiao, H. Wang and B. Tang, A fluorescence nanosensor for glycoproteins with activity based on the molecularly imprinted spatialstructure of the target and boronate affinity, *Angew. Chem., Int. Ed.*, 2014, **53**, 12489–12493.

14 Y. Ge, B. Butler, F. Mirza, S. Habib-Ullah and D. Fei, Smart molecularly imprinted polymers: recent developments and applications, *Macromol. Rapid Commun.*, 2013, **34**, 903–915.

15 X. J. Li, B. L. Zhang, W. Li, X. F. Lei, X. L. Fan, L. Tian, H. P. Zhang and Q. Y. Zhang, Preparation and characterization of bovine serum albumin surface-imprinted thermosensitive magnetic polymer microsphere and its application for protein recognition, *Biosens. Bioelectron.*, 2014, **51**, 261–267.

16 G. Pan, Q. Guo, C. Cao, H. Yang and B. Li, Thermo-responsive molecularly imprinted nanogels for specific recognition and controlled release of proteins, *Soft Matter*, 2013, **9**, 3840–3850.

17 Z. Zhang, J. H. Li, L. W. Fu, D. Y. Liu and L. X. Chen, Magnetic molecularly imprinted microsensor for selective recognition and transport of fluorescent phycocyanin in seawater, *J. Mater. Chem. A*, 2015, **3**, 7437–7444.

18 L. Cui, C. C. Li, B. Tang and C. Y. Zhang, Advances in the integration of quantum dots with various nanomaterials for biomedical and environmental applications, *Analyst*, 2018, **143**, 2469–2478.

19 J. Wang, C. X. Jiang, X. Q. Wang, L. G. Wang, A. M. Chen, J. Hu and Z. H. Luo, Fabrication of an "ion-imprinting" dual-emission quantum dot nanohybrid for selective fluorescence turn-on and ratiometric detection of cadmium ions, *Analyst*, 2016, **141**, 5886–5892.

20 Q. Yang, J. H. Li, X. Y. Wang, H. L. Peng, H. Xiong and L. X. Chen, Strategies of molecular imprinting-based fluorescence sensors for chemical and biological analysis, *Biosens. Bioelectron.*, 2018, **112**, 54–71.
21 C. Wang, Q. Ma, W. Dou, S. Kanwal, G. Wang, P. Yuan and X. Su, Synthesis of aqueous CdTe quantum dots embedded silica nanoparticles and their applications as fluorescence probes, *Talanta*, 2009, **77**, 1358–1364.
22 J. Zhou, Y. Yang and C. Y. Zhang, Toward biocompatible semiconductor quantum dots: from biosynthesis and bioconjugation to biomedical application, *Chem. Rev.*, 2015, **115**, 11669–11717.
23 J. L. Yu, X. Y. Wang, Q. Kang, J. H. Li, D. Z. Shen and L. X. Chen, One-pot synthesis of a quantum dot-based molecular imprinting nanosensor for highly selective and sensitive fluorescence detection of 4-nitrophenol in environmental waters, *Environ. Sci.: Nano*, 2017, **4**, 493–502.
24 B. Liu, F. Zeng, G. Wu, S. Wu, J. Wang and F. Tang, Ratiometric sensing of mercury(II) based on a FRET process on silica core-shell nanoparticles acting as vehicles, *Microchim. Acta*, 2013, **180**, 845–853.
25 A. Verma, O. Uzun, Y. H. Hu, Y. Hu, H. S. Han, N. Watson, S. L. Chen, D. J. Irvine and F. Stellacci, Surface-structure-regulated cell-membrane penetration by monolayer-protected nanoparticles, *Nat. Mater.*, 2008, **7**, 588–595.
26 D. Y. Li, X. W. He, Y. Chen, W. Y. Li and Y. K. Zhang, Novel hybrid structure silica/CdTe/molecularly imprinted polymer: synthesis, specific recognition, and quantitative fluorescence detection of bovine hemoglobin, *ACS Appl. Mater. Interfaces*, 2013, **5**, 12609–12616.
27 D. Sibel Emir, S. Ridvan, B. Sibel, H. Deniz, D. Adil and E. Z. Arzu, Quantum dot nanocrystals having guanosine imprinted nanoshell for DNA recognition, *Talanta*, 2008, **75**, 890–896.
28 B. T. Huy, M. H. Seo, X. F. Zhang and Y. I. Lee, Selective optosensing of clenbuterol and melamine using molecularly imprinted polymer-capped CdTe quantum dots, *Biosens. Bioelectron.*, 2014, **57**, 310–316.
29 Y. Zhou, Z. B. Qu, Y. B. Zeng, T. S. Zhou and G. Y. Shi, A novel composite of graphene quantum dots and molecularly imprinted polymer for fluorescent detection of paranitrophenol, *Biosens. Bioelectron.*, 2014, **52**, 317–323.
30 S. Rouhani and F. Nahavandifard, Molecular imprinting-based fluorescent optosensor using a polymerizable 1,8-naphthalimide dye as a florescence functional monomer, *Sens. Actuators, B*, 2014, **197**, 185–192.
31 C. Zhang, H. Y. Cui, J. R. Cai, Y. Q. Duan and Y. Liu, Development of fluorescence sensing material based on CdSe/ZnS quantum dots and molecularly imprinted polymer for the detection of carbaryl in rice and Chinese cabbage, *J. Agric. Food Chem.*, 2015, **63**, 4966–4972.
32 W. Zhang, X. He, W. Li and Y. Zhang, Thermo-sensitive imprinted polymer coating CdTe quantum dots for target protein specific recognition, *Chem. Commun.*, 2012, **48**, 1757–1759.
33 U. Athikomrattanakul, N. Gajovic-Eichelmann and F. W. Scheller, Thermometric sensing of nitrofurantoin by noncovalently imprinted polymers containing two complementary functional monomers, *Anal. Chem.*, 2011, **83**, 7704–7711.
34 D. Y. Li, Y. P. Qin, H. Y. Li, X. W. He, W. Y. Li and Y. K. Zhang, A “turn-on” fluorescent receptor for detecting tyrosine phosphopeptide using the surface imprinting procedure and the epitope approach, *Biosens. Bioelectron.*, 2015, **66**, 224–230.

